Available online at www.sciencedirect.com
ScienceDirect
International Journal of Pharmaceutics 346 (2008) 64–79
INTERNATIONAL JOURNAL OF PHARMACEUTICS
www.elsevier.com/locate/ijpharm

Partitioning, diffusivity and clearance of skin permeants in mammalian dermis

Kosmas Kretsos [1], Matthew A. Miller, Grettel Zamora-Estrada, Gerald B. Kasting *

College of Pharmacy, University of Cincinnati Academic Health Center, P.O. Box 670004, Cincinnati, OH 45267-0004, USA

Received 27 October 2005; received in revised form 1 June 2007; accepted 5 June 2007
Available online 23 June 2007

Abstract

The partition coefficients (K_{de}) and diffusivities (D_{de}) of compounds in mammalian dermis were examined through an analysis of *in vitro* permeation data obtained from the literature combined with experimental results with the test permeant, ^{3}H-testosterone. The literature data involved 26 compounds ranging in molecular weight from 18 to 476 Da and four species—human, guinea pig, rat and mouse. Testosterone was studied by permeation and desorption measurements employing excised human dermis in the presence and absence of external serum albumin. Mathematical models for both K_{de} and D_{de} were developed. The K_{de} model involved ionization, binding to extravascular serum proteins and partitioning into a small lipid compartment. The D_{de} model employed a free diffusivity with a liquid-like size dependence multiplied by a binding factor derived from K_{de}. An additional analysis considered *in vivo* dermal concentration profiles of topically applied permeants. Literature data for 5 of 6 permeants were shown to be well described by a previously published model for capillary clearance in the dermis, which leads to an exponential decay of concentration with depth. Computed decay lengths (1/*e* values) ranged from 210 to 920 μm, and the corresponding clearance rate constants k_{de} ranged from 0.9×10^{-4} to 14×10^{-4} s^{-1} ($n = 8$). Departures from the exponential decay profile are discussed in terms of non-uniform capillary clearance and incomplete attainment of a steady-state.

Keywords: Skin; In silico prediction; Mathematical model; Topical delivery; Percutaneous absorption; Transdermal

1. Introduction

The study of transport of exogenous substances within the deeper skin layers lags that of transport in stratum corneum (SC). This may be understood on the basis that the SC has long been acknowledged as the principal barrier for skin permeation. Deeper layers, including the viable epidermis and dermis, are most often lumped together and treated as a homogeneous layer (McCarley and Bunge, 2001) whose depth extends as far as the locus of the superficial dermal capillaries (Auton et al., 1994; Shah, 1996); thus, for any given skin permeant, the inherent assumption of a rapid and absolute clearance through the microcirculation in the upper dermis is effectively applied. This treatment has been followed extensively both in experimental and theoretical studies since it is simple, has proven to be adequate for many skin permeants (Scheuplein and Bronaugh, 1983), and does not require *in vivo* experimental procedures. However, the simple picture of an absolute clearance occurring at an artificially imposed boundary within the dermis is less than satisfactory for a number of problems: (a) transdermal drug delivery when the SC barrier has been seriously compromised (Amsden and Goosen, 1995; Riviere and Heit, 1997; Bauerova et al., 2001; Joshi and Raje, 2002); (b) topical application of vasoconstrictive agents (Benowitz et al., 1992; Sommer et al., 2003); (c) contact sensitization thresholds (Kimber et al., 1999) and other problems in which skin concentrations are key (Monteiro-Riviere et al., 1990, 1993); (d) effect of old age and environmental/pathological conditions on topical delivery (Flynn and Stewart, 1988; Roberts and Walters, 1998).

Experimental studies that focus on transport in the dermis *in vivo* are relatively rare. There are a few *in vivo* results available for human (Kammerau et al., 1975; Schaefer and Zesch, 1975; Zesch and Schaefer, 1975; Schaefer et al., 1978; Wagner et al., 2002), rat (Siddiqui et al., 1989; Hueber et al., 1992; Singh and Roberts, 1993a,b; Gao et al., 1995; Gupta et al., 1995) and pig

* Corresponding author. Tel.: +1 513 558 1817; fax: +1 513 558 0978.
E-mail address: Gerald.Kasting@uc.edu (G.B. Kasting).
[1] Present address: Entelos Inc., 110 Marsh Drive, Foster City, CA 94404, USA.

0378-5173/$ – see front matter © 2007 Elsevier B.V. All rights reserved.
doi:10.1016/j.ijpharm.2007.06.020

Nomenclature

Binding factor	partition coefficient multiplier in dermis accounting for solute binding to albumin and partitioning into dermis lipids
BSA	bovine serum albumin
ΔC	concentration difference across a membrane
C_{de}	dermis concentration
C_0	dermis concentration at dermal–epidermal junction
D_{aq}	aqueous diffusivity
D_{de}	effective dermis diffusivity
D_{free}	diffusivity of freely diffusing permeant in dermis
DPM	disintegrations per minute
E	exponential decay factor for dermis concentration
f_{non}	fraction non-ionized
f_u	fraction unbound to albumin
h_{de}	dermis thickness
HSA	human serum albumin
J_{ss}	steady-state flux
k_{de}	effective dermis clearance constant
k_{free}	microscopic dermis clearance constant
k_p	permeability coefficient
K_{de}	dermis/water partition coefficient
K_{free}	dermis/water partition coefficient for a non-bound solute
K_{oct}	octanol/water partition coefficient
m	mass of tissue
M	solvent molecular weight
M_{inf}	amount desorbed from tissue
MW	solute molecular weight
n	number of observations
P_{cap}	capillary permeability
P_{de}	dermis permeability ($D_{de}K_{de}$)
PBR	protein binding ratio (or fraction bound)
PBS	phosphate-buffered saline
Q	capillary blood flow rate
r^2	squared correlation coefficient (Pearson's)
R_{de}	diffusive resistance of dermis
s	root-mean-square deviation from fit
S	capillary surface area
t_L	diffusive time lag
T	temperature
V_A	molar volume at the boiling point
z_{ed}	depth of dermal–epidermal junction

Greek letters

ϕ	Wilke–Chang polarity factor
ϕ_{aq}	volume fraction of aqueous region of dermis
ϕ_{fiber}	volume fraction of fiber phase of dermis
ϕ_{lip}	lipid volume fraction of the (primarily aqueous) fluid phase of dermis
η	viscosity
ρ	density

(Monteiro-Riviere et al., 1993) skin. *In vitro* studies are more numerous and will be discussed later; the *n*-alkanols have been particularly well studied (Scheuplein, 1978; Singh and Roberts, 1996; Cross et al., 2003b). Theoretical modeling of transport within the dermis has been mostly of a compartmental nature (e.g., Guy et al., 1982; Siddiqui et al., 1989; Bookout et al., 1997; Higaki et al., 2002), an approach that provides insights as to relevant tissue levels but is difficult to generalize for new permeants. Diffusion/spatially distributed clearance approaches are limited to a rather complex, random-walk model (Kubota and Maibach, 1994) and two relatively similar models, one for isolated dermis (Gupta et al., 1995) and another for the whole skin (Kretsos et al., 2004). The latter two describe the exponential decay with depth of permeant concentration in the dermis for didanosine and salicylic acid, respectively. A diffusion-based, single-layer exponential decay scheme was also used to describe transport through full-thickness excisional wounds in rat skin (Cross and Roberts, 1999).

In this study, we first address the question of the partition coefficient (K_{de}) and diffusivity (D_{de}) of low molecular weight permeants in the dermis and the effect of protein binding and lipid partitioning on these parameters. Our conclusions are based on a literature analysis and experimental results with testosterone, a steroid hormone that is moderately protein bound in plasma. Mathematical relationships for K_{de} and D_{de} for compounds ranging in size from water (MW 18.0) to betamethasone valerate (MW 476.6) and possessing low-to-moderate degrees of protein binding are developed. We then analyze available *in vivo* skin concentration data in terms of a previously published model (Kretsos et al., 2004) which describes the relationship between transport and clearance processes in the dermis. Based on the steady-state version of the model, we characterize these processes in terms of the ratio of the volumetric, first-order, clearance rate coefficient k_{de} to the effective diffusivity D_{de}. This relationship combined with the independent mathematical model for D_{de} leads to general estimates of the magnitude of k_{de}. The key components of the dermis–permeant interaction are identified and the applicability and limitations of the present analysis are discussed. The ultimate goal of this effort is the development of a predictive tool for permeant concentration and clearance in the lower skin layers.

Nomenclature throughout the manuscript is as follows: the ratio of steady-state flux J_{ss} to concentration difference across the membrane ΔC for isolated dermis studied in a diffusion cell is the permeability coefficient k_p. For a homogeneous membrane of thickness h_{de},

$$k_p = \frac{J_{ss}}{\Delta C} = \frac{D_{de}K_{de}}{h_{de}} \quad (1)$$

where D_{de} and K_{de} have been previously defined. In experimental work, Eq. (1) is often corrected for boundary layer effects (Khalil et al., 2006). The property more directly comparable between species or between dermis preparations having different thicknesses is the permeability P_{de}, defined as

$$P_{de} = k_p h_{de} = D_{de}K_{de} \quad (2)$$

For most *in vitro* studies in which steady-state diffusion is achieved, the quantities measured include k_p, h_{de} and K_{de}. The value of D_{de} is then calculated by rearranging Eq. (2):

$$D_{de} = \frac{k_p h_{de}}{K_{de}} \tag{3}$$

In other studies the quantities measured are k_p, h_{de} and the lag time t_L for achievement of steady-state flux. In this case the value of D_{de} is estimated as

$$D_{de} = \frac{h_{de}^2}{6t_L} \tag{4}$$

The diffusive resistance of the tissue in an *in vitro* experiment is

$$R_{de}\,(\text{in vitro}) = \frac{1}{k_p} = \frac{h_{de}}{D_{de}K_{de}}. \tag{5}$$

This value should be distinguished from the effective diffusive resistance *in vivo*, which to a good approximation may be taken to be (Gupta et al., 1995; Kretsos et al., 2004)

$$R_{de}\,(\text{in vivo}) \cong \frac{1}{K_{de}\sqrt{D_{de}k_{de}}} \tag{6}$$

Eq. (6) results from the assumption of a first-order capillary clearance which is completed within the confines of the dermis.

2. Materials and methods

2.1. Materials

^{3}H-testosterone, unlabeled testosterone, bovine serum albumin (BSA), human serum albumin (HSA) and Dulbecco's phosphate-buffered saline (PBS) were obtained from Sigma Chemicals, St. Louis, MO. Microdialysis cells (1 mL and 5 mL), microdialysis membrane (Fisher 0866619, cutoff 5000 Da) and sodium azide were obtained from Fisher Scientific (Hampton, NH). Soluene-350® and Ultima Gold® XR scintillation fluid were obtained from Perkin-Elmer Life Sciences (Boston, MA). Human cadaver skin from two donors, dermatomed to a nominal thickness of 300 μm, was obtained from U.S. Tissue & Cell, Cincinnati, OH. The Donor 1 sample was back skin and the Donor 2 sample was abdominal skin. Tissue preparation and storage followed skin bank guidelines as previously described (Kasting and Bowman, 1990; Khalil et al., 2006). Isolated human dermis was obtained from these samples by heat separation (55 °C for 2 min) as described in Khalil et al. (2006).

2.2. Protein binding analysis

The binding of ^{3}H-testosterone to BSA and HSA was studied by equilibrium dialysis at 32 °C using an initial testosterone concentration of 5 μg/mL and albumin concentrations of 2% (w/v) in PBS (pH 7.4) preserved with 0.02% sodium azide. Radioactivity associated with ^{3}H-testosterone was measured by liquid scintillation counting (LSC) using a Beckman Model LS 6500 counter. Dialysis studies were conducted in glass side-by-side diffusion cells (Khalil et al., 2006) and polycarbonate dialysis cells using a dialysis membrane with a 5000 Da cutoff. Both systems gave comparable results, although equilibrium was obtained more rapidly in the polycarbonate cells due to higher surface area/volume ratios. After equilibration, unbound testosterone concentrations were approximately 1 μg/mL. Pairwise comparison of results was conducted with the Students' *t*-test (two-sided) using a significance level of $p < 0.05$.

2.3. Dermis partitioning and diffusivity measurements

Diffusivity and partition coefficient for ^{3}H-testosterone in excised human dermis were measured by two techniques, permeation and sorption/desorption (Khalil et al., 2006). All test solutions were preserved with 0.02% sodium azide. The permeation studies employed side-by-side diffusion cells (1.77 cm^2) maintained at 32 °C, with a strip of dermis mounted between donor and receiver compartments, which were stirred by star magnets driven at 600 rpm by synchronous motors. Both compartments were filled with 6 mL of either PBS, PBS + 2% BSA or PBS + 2% HSA, and the cells were allowed to equilibrate for 24 h. Skin from both donors was studied, using a total of 4–6 replicates for the PBS and PBS + 2% BSA treatments and 2 for the PBS + 2% HSA treatment. No difference between the donors was noted in this small study. To initiate the study, 100 μL of an ethanolic solution of unlabeled testosterone (300 μg/mL) and ^{3}H-testosterone (50 μCi/mL) was added to the donor chamber, yielding an initial testosterone concentration of 5 μg/mL. Aliquots (0.5 mL) of the receptor solution were collected periodically and analyzed for radioactivity by LSC. At completion of the study the dermis was dissolved in Soluene-350® (4 mL per ~1.2 g tissue) and the sample was divided into two portions. Each portion was mixed with 18 mL of scintillation fluid and analyzed by LSC. Tissue DPM were corrected for a background of 50–60 DPM and multiplied by a quench factor of 1.52 determined by adding known amounts of ^{3}H-testosterone to dissolved control tissue samples. Permeability coefficients k_p were calculated from the linear portion of a plot of cumulative amount penetrated versus time, and then corrected for boundary layer effects (Khalil et al., 2006). The correction was less than 3%. Partition coefficient K_{de} was estimated as twice the ratio of the final average radioactivity concentration in the tissue to that in the donor solution; this is equivalent to assuming a linear concentration profile in the tissue and sink conditions in the receptor compartment. The thickness h_{de} was estimated from the wet weight of the tissue using a density of 1.075 g/cm^3 (Altshuler et al., 2005). Diffusivity was calculated from Eq. (3). This method was chosen in favor of Eq. (4) due to better consistency of the flux and tissue concentration data as compared to extrapolated lag times.

The desorption studies were conducted by equilibrating a weighed sample of dermis obtained from Donor 1 (back skin) in a scintillation vial containing 5 μg/mL of testosterone and 2.5 μCi/mL of ^{3}H-testosterone in either PBS, PBS + 2% BSA or PBS + 2% HSA for 24 h at 32 °C, then sequentially desorbing the tissue samples into solutions having the same composition, but without testosterone or radioactivity. Replication was similar to the permeation studies. The tissue was dissolved in

Soluene-350® upon completion of the study, and both tissue and desorption samples were analyzed by LSC. The analysis of the desorption data followed that of Khalil et al. (2006) using the linear portion of a plot of fractional amount desorbed versus the square root of time to estimate D_{de}. K_{de} was calculated from the total amount desorbed M_{inf}, the tissue mass m and density ρ, and the equilibrium concentration of the uptake solution C_0 according to Eq. (7):

$$K_{de} = \frac{M_{inf}\rho}{mC_0}. \quad (7)$$

Pairwise comparison of diffusivity and partitioning results was conducted with the Students' t-test (two-sided) using a significance level of $p < 0.05$.

We note that protein binding, permeation and desorption studies with testosterone were conducted at 32 °C, whereas the dermis temperature *in vivo* is closer to 37 °C (Gowrishankar et al., 2004). This was an experimental limitation in our laboratory, due to concurrent work involving stratum corneum. Correction of the values obtained to 37 °C is considered in Section 4.

2.4. Analysis of diffusivity and partitioning data in dermis

Additional estimates of permeant diffusivities D_{de}, partition coefficients K_{de} and permeabilities $P_{de} = D_{de}K_{de}$ within mammalian dermis, based primarily on *in vitro* steady-state experiments, were collected from the literature (Table 1). In most cases (24 of the 27 D_{de} values reported in Table 1), the original investigators estimated the permeability coefficient k_p from steady-state flux experiments in which thickness h_{de} was also determined. They separately measured the partition coefficient K_{de} through equilibrium experiments. Diffusivity in dermis D_{de} was then calculated from Eq. (3). The remaining three values comprise our estimate derived by combining data from two different studies (methoxsalen), a previous estimate from our laboratory (salicylic acid) and a value determined in this study (testosterone). Other pertinent properties such as molecular weight, octanol/water partition coefficient, ionization constant, and fraction unbound in plasma or in albumin solutions were obtained from the literature. Molar volumes of the permeants at the boiling point, V_A, were estimated using Schroeder's method (Poling et al., 2001). These values were used to estimate the diffusivities of the permeants in water at 37 °C according to the Wilke–Chang relationship (Poling et al., 2001):

$$D_{aq}\,(\mathrm{cm^2\,s^{-1}}) = \frac{7.4 \times 10^{-8}(\phi M)^{1/2}T}{\eta V_A^{0.6}} \quad (8)$$

where $\phi = 2.26$, $M = 18.01\ \mathrm{g\,mol^{-1}}$, $T = 310\ \mathrm{K}$ and $\eta = 0.6915$ cP.

Diffusivities for the n-alkanol series studied by Scheuplein and Blank (1973) and reported again in Scheuplein (1978) were recalculated from the measured dermis permeability coefficients using the K_{de} values for the even-numbered alcohols determined later by Cross et al. (2003b). K_{de} values for the odd-numbered alcohols were interpolated from a sigmoidal curve drawn through the even-numbered K_{de} values (Cross et al., 2003b).

Further analysis of the modified dataset proceeded as follows. A physical model for solute partitioning in dermis was first developed based on the average composition of post-mortem human dermis reported by Bert et al. (1982), later modified by Bert et al. (1986). Thus, 1 g of fresh dermis was assumed to be comprised of: 650 mg of water, 300 mg of collagen, 10 mg of elastin, 11 mg of plasma proteins and a to-be-determined quantity of lipids. The lipid content was not reported by Bert, but will be shown later to be required in order to fit the partition model to experimental data for K_{de}. An upper limit to the lipid content of 0.03 $\mathrm{cm^3}$ lipid/$\mathrm{cm^3}$ dermis is provided by the average value of 27 mg/g reported earlier for post-mortem dermis by Pearce and Grimmer (1972). Taking the density of the primarily aqueous fluid phase to be 1.0 g/$\mathrm{cm^3}$ and the average density of the dermis to be 1.075 g/$\mathrm{cm^3}$ (Altshuler et al., 2005) yields an aqueous volume fraction $\phi_{aq} = (0.65\ \mathrm{g\ H_2O/g\ dermis}) \times (1\ \mathrm{cm^3\ H_2O/g\ H_2O}) \times (1.075\ \mathrm{g\ dermis/cm^3\ dermis}) = 0.70\ \mathrm{cm^3\ H_2O/cm^3}$ dermis. Most of the remaining volume consists of collagen and elastin fibers. This region is inaccessible to solutes and has volume fraction $\phi_{fiber} = 0.30$. The lipids are assigned to a small lipid compartment distributed within the aqueous phase and occupying a volume fraction ϕ_{lip} with respect to this phase. Thus, the overall lipid fraction of the dermis is $\phi_{lip}\phi_{aq}$. This definition is a matter of convenience. Both the aqueous and lipid regions are assumed to be accessible to small molecule solutes; however, there are restrictions for macromolecules as discussed below. Fig. 1 depicts the components of the dermis model.

In the absence of binding to soluble proteins or other constituents, the aqueous compartment leads to a small solute partition coefficient (relative to the non-ionized form in water)

$$K_{free} = \frac{\phi_{aq}}{f_{non}} \quad (9)$$

where f_{non} is the fraction of solute non-ionized at pH 7.4. For monofunctional acids and bases f_{non} may be estimated by the

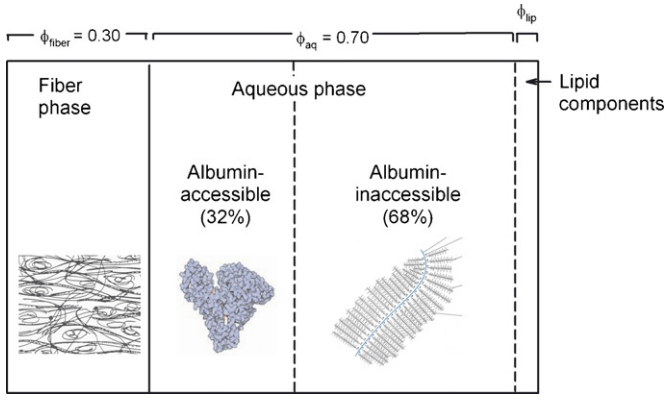

Fig. 1. Schematic diagram of dermis partitioning model based on the human dermis composition reported by Bert et al. (1982), modified to include a small lipid component. The aqueous phase (volume fraction $\phi_{aq} = 0.70$ in the diagram) is considered to be fully accessible to small molecule solutes, but only partially accessible to extravascular proteins. The glycosaminoglycans depicted in the diagram are a possible source of the excluded volume. By fitting the model in Eqs. (9)–(11) to the K_{de} data in Table 1, the final values $\phi_{aq} = 0.6$ and $\phi_{lip} = 0.001$ were selected (Eq. (20)).

Table 1
Physicochemical properties and estimated partition coefficients K_{de}, diffusivities D_{de} and permeabilities P_{de} in dermis of studied compounds

Compound	MW (Da)	V_A[a] (cm^3/mol)	log K_{oct}[b]	f_u[c]	f_u sol[d]	K_{de}[e]	$D_{de} \times 10^7$ ($cm^2\ s^{-1}$)	$P_{de} \times 10^7$ ($cm^2\ s^{-1}$)	Species	Ref.
Water	18.0	21.0	−1.38			0.7[f]	60[f]	41.7[g]	Human	g
Methanol	32.0	42.0	−0.77			0.55[f]	67[f]	36.8[g]	Human	g
Ethanol	46.1	63.0	−0.31		0.878	0.43[h]	57[f]	24.3[g]	Human	g,h
Propanol	60.1	84.0	0.25			0.43[f]	50[f]	21.5[g]	Human	g
Butanol	74.1	105.0	0.88		0.764	0.43[h]	48[f]	20.8[g]	Human	g,h
Pentanol	88.2	126.0	1.56			0.61[f]	27[f]	16.7[g]	Human	g
Hexanol	102.2	147.0	2.03		0.40	0.86[h]	16[f]	13.9[g]	Human	g,h
Heptanol	116.2	168.0	2.72			1.75[f]	9.9[f]	17.4[g]	Human	g
Octanol	130.2	189.0	3.00		0.066	3.55[h]	5.1[f]	18.1[g]	Human	g,h
Decanol	158.2	231.0	4.06		0.025	11.3[h]			Human	h
Betamethasone	392.5	423.5	2.01			2.5	7.4	18.5	Human	i
Betamethasone 17-valerate	476.6	528.5	3.60			13.6	1.6	21.8	Human	i
Methoxsalen	216.2	203.0	1.93	0.09		1.45	7.64	11.1	Human	j
Glucose	180.2	161.0	−3.24			0.65	26.4	12.8	Human	k
Testosterone	288.4	350.0	3.32	0.40	0.20	4.92[l]	4.1 ± 0.6[m]	25.4[n]	Human	–
Hydrocortisone	362.5	406.0	1.61	<0.1	0.72	2.1[o]	2.85[p]	5.2[q]	Guinea pig	r
Salicylic acid	138.1	133.0	2.26	0.1–0.2	0.14	0.9	8 ± 3		Rat	s
Pentanol	88.2	126.0	1.56			1.92	12.3	26.4	Mouse	t
Vidarabine	267.2	238.0	−1.11			1.41	9.5	13.0	Mouse	t
Vidarabine	267.2	238.0	−1.11			0.79[u]	15	12.3	Mouse	v
Hypoxanthine arabinoside	267.2	224.0	−2.31			0.81[u]	13.8	11.6	Mouse	v
Vidarabine-5-*n*-valerate	351.4	343.0	1.13			0.94[w]	9.7	9.6	Mouse	v
Progesterone	314.5	385.0	3.87		0.099	4.18	0.41 ± 0.03	1.8	Mouse	x
Desoxycorticosterone	330.5	392.0	2.88			1.64	0.53 ± 0.11	0.9	Mouse	x
11-α-Hydroxyprogesterone	330.5	392.0	2.36			1.21	0.66 ± 0.14	0.8	Mouse	x
17-α-Hydroxyprogesterone	330.5	392.0	3.17			2.64	0.62 ± 0.13	1.6	Mouse	x
Corticosterone	346.5	399.0	1.94			1.05	0.44 ± 0.08	0.5	Mouse	x
17-α-Hydroxydeoxy-corticosterone	346.5	399.0	3.08			0.85	0.64 ± 0.11	0.5	Mouse	x
Hydrocortisone	362.5	406.0	1.61	<0.1	0.72	0.65	0.44 ± 0.07	0.3	Mouse	x
Didanosine	236.2	217.0	−1.24	>0.95						y
Piroxicam	331.4	322.0	1.98	0.01	0.11					y

The experiments were performed at 37 °C and pH 7.4 unless otherwise noted. Compounds are non-ionized at pH 7.4 except for salicylic acid (weak acid, pK_a 3.0) and piroxicam (weak acid, pK_a 6.3). Didanosine (weak acid, pK_a 9.12) is about 2% ionized.

[a] Molar volume at the boiling point.
[b] log(octanol/water partition coefficient) (EpiWin Suite®, US EPA, 2006).
[c] Fraction unbound in plasma (Pibouin et al., 1987; Wheeler, 1995; Roberts and Cross, 1999; Moffat et al., 2003).
[d] Fraction unbound in a 2% (Singh and Roberts, 1996) or 4% (Cross et al., 2003a) solution of serum albumin.
[e] Direct measurement unless otherwise stated, expressed as $K_{de/pH\,7.4}$ (Eq. (13)).
[f] Our calculation as described in text.
[g] Scheuplein and Blank (1973), P_{de} measured at 25 °C.
[h] Cross et al. (2003b), room temperature.
[i] Kubota and Maibach (1993). Experiments performed at pH 4.5. K_{de} calculated from initial/equilibrium solution concentration difference.
[j] Estimate based on an *in vivo* (Kammerau et al., 1976) and an *in vitro* (Anigbogu et al., 1996) study ($T = 32$ °C), calculation available on request.
[k] Khalil et al. (2006). $T = 32$ °C.
[l] Average of permeation and desorption methods, PBS treatment only.
[m] Average of all treatments and methods.
[n] Permeation study with PBS treatment only.
[o] Dermis/aqueous buffer value.
[p] Calculated from P_{de} and a K_{de} value from Myglyol 480.
[q] Stripped skin value used and adjusted for thickness. Myglyol 480 vehicle.
[r] Borsadia et al. (1992).
[s] Estimate from *in vivo* study (Kretsos et al., 2004).
[t] Yu et al. (1980). D_{de} value calculated from Eq. (4), K_{de} from P_{de}/D_{de}.
[u] Calculated from solution concentration change.
[v] Yu et al. (1979). Experiments performed at pH 4.5.
[w] Calculated as average of P_{de}/D_{de}.
[x] Tojo et al. (1987).
[y] Data for these compounds included for calculations in Table 2.

usual formulas (Florence and Attwood, 2006):

$$f_{non} = \begin{cases} \dfrac{1}{1+10^{7.4-pK_a}}, & \text{weak acid} \\ \dfrac{1}{1+10^{pK_a-7.4}}, & \text{weak base} \end{cases} \quad (10)$$

For polyfunctional compounds f_{non} may be estimated by more sophisticated formulas. A useful program incorporating such calculations is ACD/logD^{TM} (ACD Labs Inc., www.acdlabs.com). Eq. (9) is predicated on the assumption that there is no charge exclusion for small solutes in the dermis. Since charge exclusion is known to be a factor for albumin (Wiig et al., 2003), this assumption warrants careful evaluation.

Based on equilibrium partitioning of radiolabeled albumin, Bert et al. (1982) considered the albumin-accessible and albumin-inaccessible regions of the fluid fraction of dermis to be proportioned in the ratio of 0.32:0.68. The concentration of albumin in the albumin-accessible region was originally estimated to be ~5% (Bert et al., 1982), but was later measured to be 0.45–0.93 (mean 0.68) of the serum concentration (Bert et al., 1986). Taking the serum concentration to be 0.6 mM or 4.0% (w/v) for this 67.4 kDa protein (Kratochwil et al., 2002) yields $0.68 \times 4.0\% = 2.7\%$ (w/v). We assumed that a solute will partition into the albumin-inaccessible aqueous region with a partition coefficient (with respect to the non-ionized form in water) of $1/f_{non}$, into the albumin-accessible fluid region with a partition coefficient of $1/(f_u f_{non})$, where f_u is the fraction unbound, and into the lipid region with a partition coefficient equal to the octanol–water partition coefficient K_{oct}. Combining these assumptions with Eq. (9) leads to a calculated dermis partition coefficient of:

$$K_{de/non} = K_{free}\left(0.68 + \frac{0.32}{f_u} + \phi_{lip} f_{non} K_{oct}\right) = K_{free} \cdot \text{Binding factor} \quad (11)$$

where f_u is the fraction unbound in a 2.7% albumin solution at pH 7.4. The reference state ("non") for Eq. (11) is an aqueous solution in which the solute is completely non-ionized. The quantity in parentheses is identified as the solute binding factor in dermis. It will appear regularly in the subsequent analysis. For a small, non-protein bound, hydrophilic solute like glucose, the binding factor is 1. This factor also distinguishes the freely diffusing concentration C_{free} from the total concentration C_{de}. Thus,

$$C_{de} = C_{free} \cdot \text{Binding factor} \quad (12)$$

K_{de} may alternatively be expressed relative to a pH 7.4 buffer as

$$K_{de/pH\,7.4} = f_{non} K_{de/non} \quad (13)$$

Eq. (11) applies to the case in which a non-ionized solute or solution thereof is applied topically to full-thickness skin. Eq. (13) is appropriate for interpreting *in vitro* experiments in which the dermis is contacted by an aqueous buffer solution maintained at pH 7.4.

Values of the unbound fraction f_u for the permeants studied were either obtained from the literature (Pibouin et al., 1987; Wheeler, 1995; Roberts and Cross, 1999; Moffat et al., 2003; Singh and Roberts, 1996; Cross et al., 2003a) or calculated from the mathematical model described by Yamazaki and Kanaoka (2004). The value of f_u so calculated is equal to 1 − PBR in the original notation, where PBR stands for "protein binding ratio" and is equivalent to fraction bound. No attempt was made to correct the values so obtained to an albumin concentration of 2.7%. This decision was based on the considerable uncertainties in both the f_u estimation method and the 2.7% target concentration.

Dermis lipids are largely associated with cell membranes and may be considered to be immobile. Although it has some mobility in the dermis, albumin moves more slowly than small solutes due to its size. Thus, for weakly and moderately bound solutes, to a first approximation, it too may be considered to be immobile. The combined effect of binding and partitioning on the diffusivity of mobile solutes is thus (Cussler, 1997; Kasting et al., 2003)

$$D_{de} = \frac{D_{free}}{\text{Binding factor}} \quad (14)$$

where D_{de} is the observed or effective diffusivity and D_{free} is the diffusivity in the absence of binding or partitioning. In deriving Eq. (14) it is assumed that D_{free} has the same value for ionized and non-ionized solute. The permeability of the tissue is given by

$$P_{de} = D_{de} K_{de} = D_{free} K_{free} \quad (15)$$

Note that, to the extent that albumin and dermal lipids may be considered to be immobile, the permeability is independent of binding and partitioning, as it must be at steady-state (Cooper, 1974; Kasting et al., 2003). A more detailed analysis of dermis diffusivity would include the motion of solute bound to albumin. This elaboration will probably be required in order to explain the transport of very highly protein bound solutes.

2.5. Analysis of in vivo skin concentration data

A summary of the *in vivo* skin permeation studies that were analyzed is shown in Table 2. In these studies, radiochemical detection was used except by Gao et al. (1995) and Gupta et al. (1995) where samples were analyzed by HPLC. A specified dose was applied, confined to a specific skin surface area by external means in order to avoid spreading. After a time lapse (Table 2) the skin surface was rinsed and dried, and skin biopsies were obtained. The biopsies were immediately frozen and subsequently microtomed to obtain 10–60 μm thick sections. The samples were analyzed to yield concentration as a function of depth. The amount of replication varied widely between studies (Table 2).

The data were analyzed according to the distributed diffusion-clearance model reported previously (Kretsos et al., 2004). Briefly, the model addresses transient one-dimensional skin permeation from a finite or infinite dose with all the skin strata explicitly represented. Capillary clearance is represented by a uniform removal rate equal to k_{de} times the local concentration C_{de} at all points in the dermis. In this paper, we consider its steady-state solution for an infinite dose application with no

Table 2
In vivo studies of skin concentrations of topically applied permeants

Fig. 5 panel	Permeant	Species/site	n[a]	Time[b] (min)	$\ln C_0$	E (cm^{-1})[a]	$D_{de} \times 10^7$ ($cm^2\ s^{-1}$)[b]	$k_{de} \times 10^4$ (s^{-1})	$k_{free} \times 10^4$ (s^{-1})	Ref.
a	Hydrocortisone	Human	1	1000	-7.01 ± 0.17	43.0 ± 3.9	7.7	14.2	16.6	[c]
b	Retinoic acid	Human	1	100	–	–	–	–	–	[d]
c	Methoxsalen	Human/breast[e]	1	100	-11.05 ± 0.16	20.8 ± 2.0	9.0	3.9	16.8	[f]
d	Piroxicam	Yorkshire pig/dorsal	8	720	10.76 ± 0.10	12.8 ± 1.0	5.4	0.9	3.2	[g]
e	Hydrocortisone	Hairless rat/dorsal	4	360	2.17 ± 0.59	37.5 ± 13.0	7.7	10.8	12.6	[h]
f	Testosterone	Hairless rat/dorsal	4	360	5.10 ± 0.36	48.2 ± 8.0	2.2	5.1	22.3	[h]
g	Didanosine	Fisher rat/dorsal[i]	7	360	0.58 ± 0.06	10.9 ± 0.6	19.4	2.3	2.3	[j]
h	Didanosine	Fisher rat/dorsal	6	360	1.76 ± 0.07	23.0 ± 0.8	19.4	10.3	10.4	[k]
–	Salicylic acid	Wistar rat/dorsal	3	120	–	–	8 ± 3[l]	7 ± 2[l]	20.8	[m]

The concentration data and regression analyses are shown in Fig. 6. Regression constants $\ln C_0$ and E and were calculated from these data according to Eq. (17). D_{de} was derived from Eqs. (14), (20) and (21) and k_{de} was calculated as $D_{de}E^2$. Regression results are presented as mean ± the standard parameter error.

[a] Number of subjects (one experiment was performed per subject).
[b] Time of tissue collection post-application.
[c] Zesch and Schaefer (1975).
[d] Schaefer and Zesch (1975).
[e] Measurement prior to UV irradiation.
[f] Schaefer et al. (1978).
[g] Monteiro-Riviere et al. (1993).
[h] Hueber et al. (1992).
[i] The hair was clipped.
[j] Gupta et al. (1995).
[k] Gao et al. (1995).
[l] Value from Kretsos et al. (2004).
[m] Singh and Roberts (1993b). This study was performed on de-epidermized skin.

direct transport beyond the lower boundary of the dermis, i.e., the dermis is assumed to be semi-infinite. This solution yields for the dermis an exponential decay of concentration with depth,

$$C_{de} = C_0 \cdot \exp\left[-\sqrt{\frac{k_{de}}{D_{de}}}(z - z_{ed})\right] = C_0 \cdot \exp\left[-E(z - z_{ed})\right] \quad (16)$$

or

$$\ln C_{de} = \ln C_0 - \sqrt{\frac{k_{de}}{D_{de}}}(z - z_{ed}) = \ln C_0 - E(z - z_{ed}) \quad (17)$$

where the decay parameter is $E = \sqrt{k_{de}/D_{de}}$. The sign of the depth variable z in Eqs. (16) and (17) is chosen such that more positive values reflect increasing depth in the tissue. The skin surface is taken to be at depth $z = 0$. The pre-exponential factor, C_0, corresponds to the dermis concentration just below the dermal–epidermal junction located at depth z_{ed}, whose average value was taken to be equal to 100 μm. The value of C_0 depends on the properties of all layers, i.e., donor solution, stratum corneum, viable epidermis, and dermis (Kretsos et al., 2004). The decay parameter E, which is the inverse of the decay length, depends solely on properties of the dermis and can be calculated from the available data. Thus, a linear regression analysis of the available *in vivo* skin concentration data was performed based on Eq. (17). The regression coefficients, 95% confidence intervals and coefficients of variance were calculated with SigmaStat 3.10©(Systat Software Inc., Richmond, CA, U.S.A.).

Consistent with the partitioning and diffusivity models (Eqs. (9)–(14)), it is appropriate to consider k_{de} as an effective parameter that is related to a microscopic clearance parameter k_{free} according to

$$k_{de}C_{de} = k_{free}C_{free} \quad (18)$$

where C_{free} is the value defined by Eq. (12). This follows because the intrinsic clearance rate must be proportional to the freely diffusing concentration C_{free} rather than the total concentration C_{de}. Comparing Eqs. (12) and (18) one finds

$$k_{de} = \frac{k_{free}}{\text{Binding factor}} \quad (19)$$

The microscopic parameter k_{free} is more likely to be relatable to capillary bed properties than is the effective parameter k_{de}.

3. Results

3.1. Testosterone protein binding

The partition coefficient between PBS and PBS + 2% BSA for radioactivity associated with ^{3}H-testosterone in the side-by-side diffusion cells was 3.44 ± 0.14 ($n = 3$), and the corresponding value for 2% HSA was 4.02 ± 0.26 ($n = 3$). These values translate into unbound fractions $f_u = 0.29 \pm 0.01$ for testosterone in 2% BSA and $f_u = 0.25 \pm 0.02$ for testosterone in 2% HSA. While statistically significant, these small differences between bovine and human albumins would not be expected to have a functional consequence. The polycarbonate cells yielded $f_u = 0.34 \pm 0.07$ ($n = 2$) for testosterone in 2% BSA, which was not significantly different from the side-by-side cell result for this solution. All of our values fall between the value $f_u = 0.2$ reported by Singh and Roberts (1996) for testosterone in a 2% albumin solution and the value $f_u = 0.40$ for testosterone in plasma reported by Dollery (1999).

Table 3
Partition coefficient and diffusivity of ^{3}H-testosterone in dermis

Composition	n	$K_{de/pH\,7.4}$	$D_{de} \times 10^7$ (cm^2 s^{-1})
Permeation			
PBS	4	6.37 ± 0.88	4.43 ± 1.18
PBS + 2% BSA	5	2.65 ± 0.48	4.14 ± 0.78
PBS + 2% HSA	2	1.77 ± 0.54	3.66 ± 0.02
Desorption			
PBS	4	5.65 ± 5.06	3.82 ± 1.30
PBS + 2% BSA	6	1.08 ± 0.20	5.25 ± 1.43
PBS + 2% HSA	2	1.10 ± 0.09	3.53 ± 0.95
Mean ± S.D. (all determinations)			4.1 ± 0.6

3.2. Testosterone partitioning and diffusivity in dermis

Results of the permeation and desorption experiments with ^{3}H-testosterone in dermis are shown in Table 3 and Fig. 2. The two methods gave comparable values for diffusivity and partitioning, with only the K_{de} value for testosterone in PBS + 2% BSA showing a significant difference between permeation and desorption. There were no significant differences between the calculated D_{de} values of any of the treatment groups. Thus, we did not distinguish an effect of external serum albumin on the diffusivity of testosterone in the tissue. The average value of these measurements over all treatments and methods of $D_{de} = (4.1 \pm 0.6) \times 10^{-7}$ cm^2 s^{-1} is used for later analysis.

The partition coefficient K_{de} for testosterone between dermis and the bathing solution was 3 to 5-fold lower in the presence of external albumin than in its absence. These differences were significant for the permeation experiments, but not for desorption. There were no differences between K_{de} for BSA and HSA solutions. The ratio of K_{de} in the absence and presence of external albumin was similar to the partition coefficient between albumin and PBS solutions in the equilibrium dialysis study (Section 3.1). Tissue radioactivity at the end of the desorption study was about 15% of the total sorbed.

3.3. Permeant partitioning and diffusivity in dermis (literature data)

Physical properties and calculated values of partition coefficient (with respect to donor solution) K_{de}, diffusivity D_{de}, and permeability P_{de} in dermis for the studied compounds are shown in Table 1. Four mammalian species – human, guinea pig, rat and mouse – are represented. Molecular weight ranged

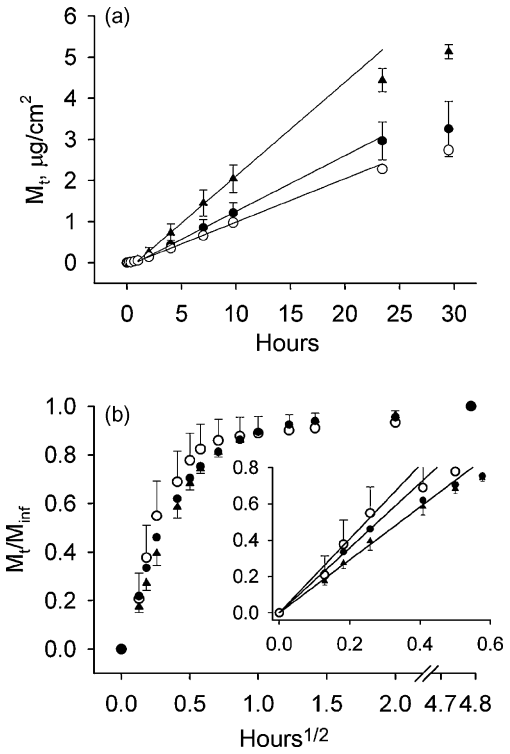

Fig. 2. Results of dermal transport studies with ^{3}H-testosterone (mean ± S.D.). (a) Permeation data, $n = 2$–5. (b) Desorption data, $n = 2$–6. The inset shows the initial part of the curves. Key: (▲)PBS; (●) PBS + 2% BSA; (◯) PBS + 2% HSA. For desorption, the average values of M_{inf} for the three treatments, respectively, were 17.8, 3.78 and 4.00 µg/cm^3 of tissue. The solid lines show the result of linear regression analyses leading to the parameters in Table 3.

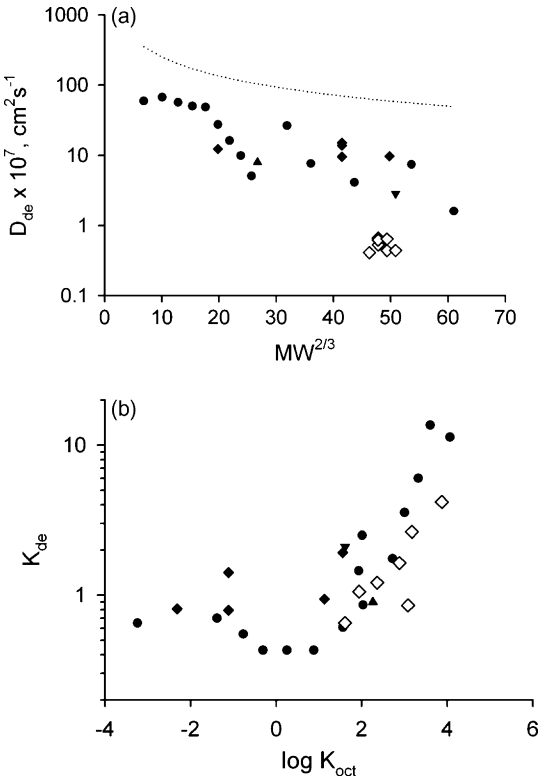

Fig. 3. (a) Diffusivity and (b) partition coefficient with respect to donor solution of permeants in mammalian dermis (data from Table 1). Key: (●) human; (▼) guinea pig; (▲)rat; (♦) mouse (Yu et al., 1979, 1980); (◊) mouse (Tojo et al., 1987). The dotted line approximates the Wilke–Chang relationship for diffusivity in water at 37 °C (Eq. (8)) as described in the text.

from 18 Da (water) to 477 Da (betamethasone valerate) and log (octanol/water partition coefficient) ranged from −3.24 (glucose) to 4.06 (decanol). Protein binding propensity, expressed as fraction unbound in either plasma or albumin solutions, varied over a wide range. Two of the compounds (salicylic acid and piroxicam) are extensively ionized at physiologic pH; hence, the concentrations in dermis are modified by ionization as may be seen from Eqs. (9)–(12).

Initial examination of these data showed that D_{de} values were strongly correlated with the size of the permeants, expressed in Fig. 3a as MW$^{2/3}$. This observation accords with expectations for diffusivities in either liquids (Poling et al., 2001) or tissues (Potts and Guy, 1992). The plot suggests a rather steep dependence of diffusivity on size compared to that expected in water (dotted line). The *n*-alkanol diffusivities, recalculated as described in Section 2.4, fell rapidly with increasing MW, while the diffusivity values of Tojo et al. (1987) for steroids in mouse dermis (open diamonds) lay well below the rest of the dataset. The latter values were obtained on tape-stripped skin rather than isolated dermis and with 40% PEG 400 donor and receiver solutions rather than water or aqueous buffer. Our own experience with this method (Khalil et al., 2006) shows that artificially low values of dermis permeability may be obtained from such preparations, probably due to incomplete removal of the stratum corneum. Hence, we consider Tojo's D_{de} values to be unreliable. However, we show later that they can be brought into closer accord with the remaining data by considering the effect of binding and partitioning.

K_{de} values were related to octanol/water partition coefficient in a non-linear manner (Fig. 3b). An average value of $K_{de} \cong 0.6$ was observed for non-ionized compounds having log $K_{oct} < 2$. For higher values of log K_{oct}, K_{de} values rose sharply to a maximum value of 13.6 (betamethasone valerate). K_{de} values for the steroids in Tojo et al.'s (1987) study showed a similar dependence on log K_{oct}, but lay below the other values. The lower values may be understood on the basis of the non-aqueous solutions employed in this study. Consequently, neither the D_{de} or K_{de} data from Tojo et al. (1987) were included in the following analyses.

According to the model presented in Section 2.4 and summarized in Eqs. (9)–(12), the increase in K_{de} with increasing solute lipophilicity shown in Fig. 3b results from two factors—binding to extravascular albumin and partitioning into dermis lipids. Since these two factors are correlated (Kratochwil et al., 2002; Yamazaki and Kanaoka, 2004) and the existing data are sparse, their rigorous deconvolution was not possible in the present analysis. An estimation of the relative contribution of the two factors was made as follows. Fraction unbound f_u was calculated for each permeant using the method of Yamazaki and Kanaoka (2004). The results are tabulated in Table 4. The value $\phi_{aq} = 0.6$ was then selected to fit Eq. (9) to the K_{de} values for hydrophilic permeants (Fig. 3b). Next the parameter ϕ_{lip} in Eq. (11) was

adjusted to achieve a suitable correspondence with the experimental values of K_{de} for lipophilic permeants. The result was $\phi_{lip} = 0.001$. These two choices yielded an explicit form for Eqs. (9)–(11), i.e.,

$$\text{Binding factor} = 0.68 + \frac{0.32}{f_u} + 0.001 f_{non} K_{oct}$$
$$K_{de/non} = \frac{0.6}{f_{non}} \cdot \text{Binding factor} \quad (20)$$

The fit to the K_{de} data provided by Eq. (20) was of comparable quality to that resulting from a non-linear regression analysis of Eqs. (9)–(11), expressed as base 10 logarithms, against the experimental values of log K_{de}. The regression analysis (not shown) yielded a slightly lower value of ϕ_{aq} and a slightly higher value of ϕ_{lip} than did the sequential fitting procedure. Statistical analysis of both fits yielded $n = 22$, $s = 0.22$ and $r^2 = 0.76$, where n is the number of observations, s the root-mean-square deviation of the data points from the fitted line and r^2 is the coefficient of determination, equal to the square of Pearson's correlation coefficient r. A plot of this relationship is shown in Fig. 4a. Values of the binding factors and K_{de} calculated from Eq. (20) are shown in Table 4. While the agreement displayed indicates the experimental values are satisfactorily described by Eq. (20), it does not guarantee that the absolute K_{de} values are correct for *in vivo* analyses, as will be discussed. Furthermore, the analysis did not unequivocally establish the significance of the parameter ϕ_{lip}. A fit with $\phi_{lip} = 0$ yielded a 17% increase in the sum of squared residuals versus Eq. (20), and the associated probability of $\phi_{lip} = 0$ based on random variation in the dataset was $p = 0.15$. The primary advantage of the choice $\phi_{lip} = 0.001$ was better agreement of Eq. (20) with the K_{de} values for the two most lipophilic permeants, betamethasone valerate and decanol.

If the increase in K_{de} with increasing lipophilicity is due to binding to relatively immobile but non-contiguous constituents of the dermis, as we have postulated, then it follows logically that the effective dermis diffusivities D_{de} must be related to lipophilicity in an inverse manner (cf. Eq. (14)). Consequently, we employed Eq. (20) in conjunction with Eq. (14) to estimate values of D_{free} from the D_{de} values in Table 1. The results of this calculation are shown in Table 4 and Fig. 4b. D_{free} values so calculated were still related to MW in an inverse fashion, but the dependence was weaker than that for D_{de}. A linear regression

Table 4
Calculated fractions unbound, binding factors, partition coefficients K_{de}, diffusivities D_{de} and permeabilities P_{de} in dermis of studied compounds

Compound	f_u[a]	Binding factor (Eq. (20))	$K_{de/pH\,7.4}$ (Eqs. (13) and (20))	$D_{free} \times 10^7$ ($cm^2\,s^{-1}$; Eq. (21))	$P_{de} \times 10^7$ ($cm^2\,s^{-1}$; Eq. (15))
Water	0.863	1.05	0.63	106.6	64.0
Methanol	0.783	1.09	0.65	73.1	43.9
Ethanol	0.700	1.14	0.68	57.6	34.5
Propanol	0.576	1.24	0.74	48.4	29.0
Butanol	0.423	1.44	0.87	42.2	25.3
Pentanol	0.272	1.89	1.14	37.6	22.6
Hexanol	0.190	2.47	1.48	34.2	20.5
Heptanol	0.105	4.24	2.54	31.4	18.9
Octanol	0.082	5.59	3.35	29.2	17.5
Decanol	0.030	22.84	13.70	25.7	15.4
Betamethasone	0.193	2.44	1.46	14.2	8.5
Betamethasone 17-valerate	0.047	11.52	6.91	12.5	7.5
Methoxsalen	0.206	2.32	1.39	20.9	12.6
Glucose	0.961	1.01	0.61	23.6	14.1
Testosterone	0.061	8.03	4.82	17.3	10.4
Hydrocortisone	0.263	1.94	1.16	14.9	8.9
Salicylic acid	0.113	3.51	2.10	28.1	16.8
Didanosine	0.950	1.02	0.61	19.7	11.8
Pentanol	0.272	1.89	1.14	37.6	22.6
Vidarabine	0.832	1.06	0.64	18.2	10.9
Vidarabine	0.832	1.06	0.64	18.2	10.9
Hypoxanthine arabinoside	0.931	1.02	0.61	18.2	10.9
Vidarabine-5-*n*-valerate	0.364	1.57	0.94	15.2	9.1
Progesterone	0.036	16.98	10.19	16.4	9.8
Desoxycorticosterone	0.091	4.94	2.97	15.8	9.5
11-α-Hydroxyprogesterone	0.144	3.13	1.88	15.8	9.5
17-α-Hydroxyprogesterone	0.070	6.73	4.04	15.8	9.5
Corticosterone	0.204	2.34	1.40	15.4	9.2
17-α-Hydroxydeoxy-corticosterone	0.076	6.09	3.66	15.4	9.2
Hydrocortisone	0.263	1.94	1.16	14.9	8.9
Piroxicam	0.143	2.92	1.75	15.8	9.5

K_{de} and P_{de} are calculated with respect to pH 7.4 buffer for comparison to the data in Table 1.
[a] Calculated by method of Yamazaki and Kanaoka (2004).

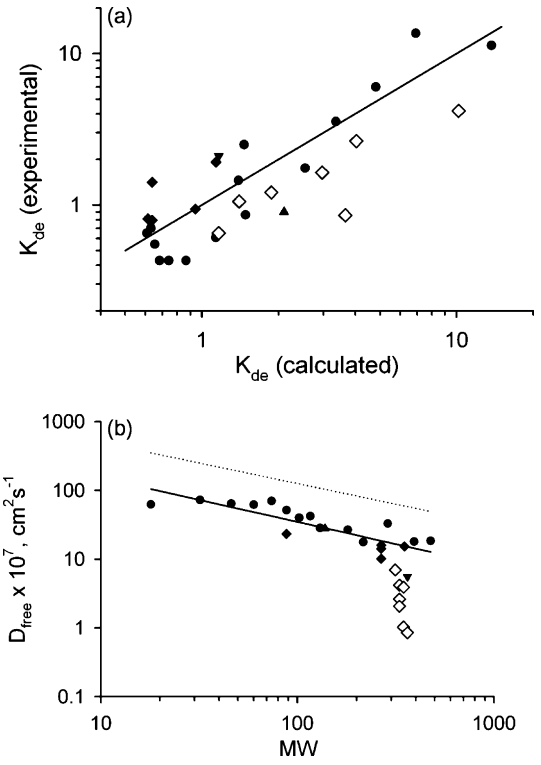

Fig. 4. (a) Experimentally determined dermis/buffer partition coefficients plotted vs. those calculated from Eq. (20). The solid line is the line of perfect fit. (b) Calculated diffusivity of Table 1 permeants in the absence of binding and partitioning. The solid line represents Eq. (21) and the dotted line approximates the Wilke–Chang correlation. The symbols are the same as those in Fig. 3.

of the data in Fig. 4b versus molecular weight, excluding those from Tojo et al. (1987), yielded

$$\log D_{\text{free}} = -4.15 - 0.655 \log \text{MW}$$
$$n = 21, \qquad s = 0.176, \qquad r^2 = 0.682 \tag{21}$$

No improvement in the correlation was found by substituting V_A for MW. Indeed, these parameters are themselves highly correlated—for the present data subset, $V_A = 1.057$ MW ($r^2 = 0.937$). Other relationships consistent with the data in Fig. 4b may be found. For example, a regression of log D_{free} versus $\text{MW}^{1/3}$ yields $r^2 = 0.698$ and $s = 0.172$. Such a relationship would suggest a steeper dependence of D_{free} on MW than that predicted by Eq. (21). It is not possible to ascertain from these data alone the exact functional form; consequently, extrapolation of Eq. (21) beyond the molecular weight range examined in this study (18–477 Da) should be done cautiously. The size dependence described by Eq. (21) ($D_{\text{free}} \propto \text{MW}^{-0.655}$) is close to that for aqueous diffusivity (Eq. (8)). The uncertainty in the slope (-0.655 ± 0.103) contains within it the Wilke–Chang value of -0.6. Hence, it may be stated that the D_{free} values in Fig. 4b are equivalent to aqueous diffusivities divided by a factor of approximately 3.7.

Assuming the stripped skin values from Tojo et al. (1987) can be dismissed, there is little evidence in Fig. 4b for species differences in the value of D_{free}. The uncertainty in D_{free} relative to the prediction from Eq. (21) increases with molecular weight,

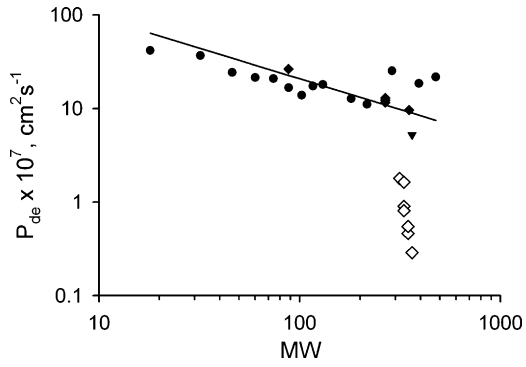

Fig. 5. Permeability $P_{de} = D_{de}K_{de}$ of solutes in the dermis. The experimental data are from Column 9 of Table 1. The solid line represents the values of P_{de} calculated from Eq. (15) (Table 4, Column 6). The symbols are the same as those in Fig. 3.

most likely reflects the increasing influence of binding and partitioning on the experimental measurements—factors that are only approximately accounted for by Eq. (14).

Fig. 5 shows that experimental dermis permeability values P_{de} (Table 1) decreased steadily with increasing molecular weight of the permeant. The trend was reasonably well described by the model calculation, $P_{de} = K_{\text{free}}D_{\text{free}}$ (Eq. (15)), bearing in mind that the partition coefficients for this comparison are expressed relative to pH 7.4 buffer. The slight lack of fit of the model to the data may arise because the experimental datasets for K_{de}, D_{de} and P_{de} were comprised of slightly different subsets of the compounds in Table 1. It may be stated that the correspondence for P_{de} is satisfactory.

3.4. *In vivo* skin concentration profiles and capillary clearance

The results of the analysis of *in vivo* skin concentration data are shown in Fig. 6 and Table 2. The distributed clearance model (Eq. (16) or (17)) predicts an exponential decay of concentration with depth for compounds that are cleared uniformly in the dermis. Fig. 6 shows that most of the measured concentration profiles correspond reasonably well to this model. The average coefficient of determination (r^2) for linear regressions according to Eq. (17) was 0.81, and half of the studied compounds yielded $r^2 > 0.88$. Retinoic acid (Fig. 6b, $r^2 = 0.486$) was an exception. This compound was excluded from further investigation due to the poor representation of the data by Eq. (17). The issue is addressed further in Section 4.

Exponential decay factors, $E = \sqrt{k_{de}/D_{de}}$, derived from this analysis are shown in Table 2. Values of E ranged from $(10.9 \pm 0.6)\,\text{cm}^{-1}$ for didanosine in rat to $(48.2 \pm 8.0)\,\text{cm}^{-1}$ for testosterone in rat. The single human value was $(43.0 \pm 3.9)\,\text{cm}^{-1}$ for hydrocortisone. These values translate into characteristic lengths of 210–920 μm for a 1/*e*-fold fall in concentration. Examination of Fig. 6 shows that several of the studies (Panels b, d, e, f and h) would support a more gradual decrease of concentration with depth in the lower dermis. Such profiles would be expected if clearance in this region were lower than in the papillary dermis. This possibility, which may be antic-

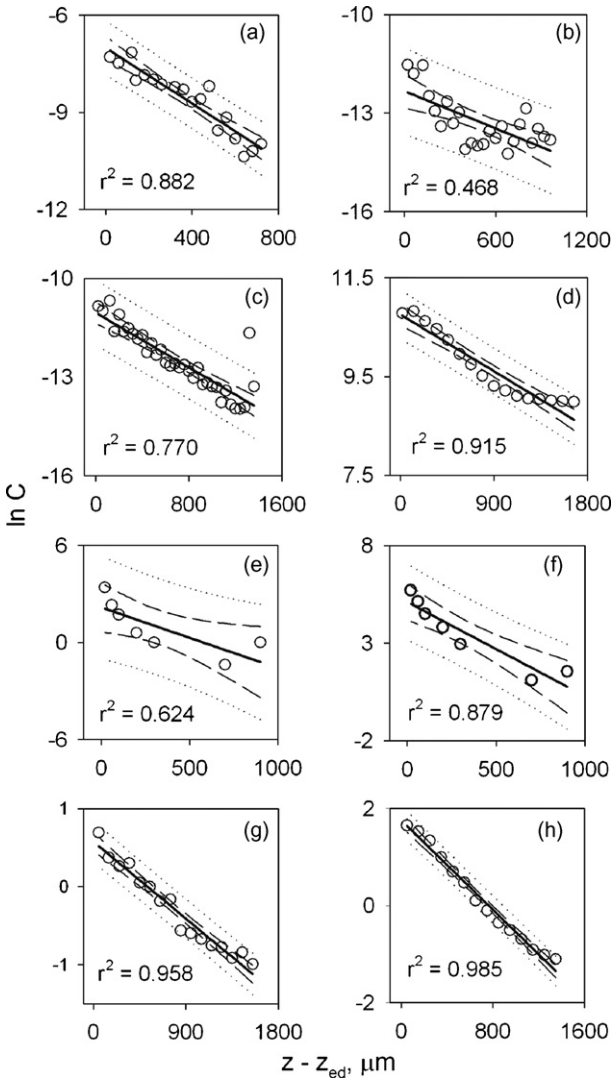

Fig. 6. *In vivo* skin concentration vs. depth profiles taken from the studies listed in Table 2. The points represent the mean of 1–8 experiments as shown in the table. Panels (a–c) show human skin data, (d) is pig and (e–h) are rat. Solid lines, linear regression; dotted lines, prediction interval; dashed lines, 95% confidence interval. (a) Hydrocortisone (mol/L); (b) retinoic acid (mol/L); (c) methoxsalen (mol/L); (d) piroxicam (DPM/section); (e) hydrocortisone (nmol eq/cm^3); (f) testosterone (nmol eq/cm^3); (g) didanosine (mg/g); (h) didanosine (mg/g).

ipated from studies of skin microvasculature (Braverman, 1997), leaves open the possibility of concentration profiles extending into the underlying fat and muscle layers, as recently reviewed by Lee and Maibach (2006).

Deconvolution of the k_{de} values according to Eqs. (1) and (20) yielded the k_{free} values shown in Table 2. There was a trend toward increasing values of k_{free} with increasing lipophilicity of the non-ionized solute, as shown in Fig. 7. The trend was not as apparent when the solute octanol/water distribution coefficient, equivalent to $f_{non}\ K_{oct}$, was substituted for the partition coefficient K_{oct} in Fig. 7. This occurred because salicylic acid, which has a high value of k_{free}, has a high partition coefficient but a low distribution coefficient at pH 7.4. Implications of these relationships are discussed later.

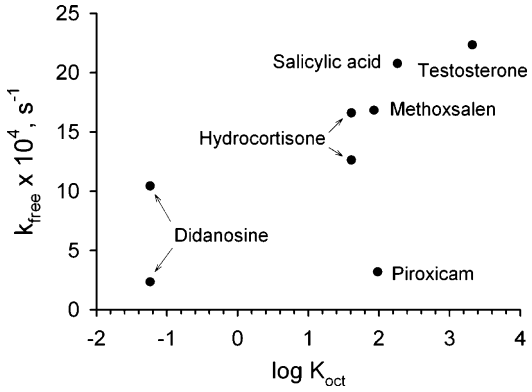

Fig. 7. Microscopic clearance constant $k_{free} = k_{de}$·Binding factor (cf. Eq. (19)) of solutes in the dermis, plotted vs. octanol/water partition coefficient of the non-ionized solute. Values of k_{de} are listed in Table 2 and the binding factors are calculated in Table 4.

4. Discussion

Estimation of skin and deep tissue concentrations of topically applied compounds plays an important role in the development of new topical drug therapies, whether they are intended for skin or for underlying muscles and joints (Siddiqui et al., 1989; Singh and Roberts, 1993a, 1996). It also provides key information related to skin toxicities including irritant and allergic contact dermatitis (Kimber et al., 1999). Unlike systemic percutaneous absorption, which is usually dominated by the barrier properties of stratum corneum, skin concentrations always reflect a balance of permeation through the stratum corneum, partitioning, diffusion and (sometimes) metabolism in the viable skin layers and capillary clearance in the dermis. Hence, a good understanding of transport properties of epidermis and dermis is essential to predicting skin concentration profiles.

Considerable progress has been made toward interpreting skin and lower tissue concentrations in terms of compartmental pharmacokinetic models, as outlined in the Introduction. This approach meshes well with systemic pharmacokinetic descriptions of drug distribution and transport; however, it is more effective for interpretation of existing data than for prediction of the skin concentration profile of a new substance. The diffusion-based approach described herein represents an alternative to compartmental models that can be more directly related to transport properties of the tissue and the physicochemical properties of the permeant. Consequently, it has more potential as a predictive tool than does the well-stirred compartment approach.

Considering each layer of the skin to be a homogeneous medium with an associated loss mechanism (e.g., capillary clearance or metabolism), three properties within the layer are required to describe diffusive transport *in vivo*—a partition coefficient, K; a diffusivity, D; and a clearance constant k. These parameters are discussed, in turn, below. Eqs. (5) and (6) show the way in which these parameters combine to yield the diffusive resistance of the dermis R_{de} for *in vitro* and *in vivo* studies, respectively, when k_{de} is interpreted purely as capillary clearance.

Partition coefficients K_{de} for solutes between dermis and buffer solutions were clearly related to the lipophilicity of the solute (Fig. 3b). We have described this behavior in terms of a model in which the solute binds reversibly to extravascular serum proteins (primarily albumin) and partitions into dermis lipids (Eqs. (9)–(12) and (20)). The latter are loosely interpreted as including both the cell membranes associated with the dermis cellular constituents and lipids associated with the pilosebaceous unit, which is more accurately described as an invagination of the epidermis into the dermis. However, for a diffusion model employing a slab geometry, the pilosebaceous lipids are spatially associated with the dermis layer. The binding model adequately described K_{de} values obtained from *in vitro* experiments employing isolated dermis from four mammalian species (Fig. 4a). However, it should be noted that the methodology for these studies involved immersion of the tissue in aqueous buffer solutions. Diffusible protein within the tissue may have equilibrated with the external solutions, leading to calculated K_{de} values lower than the effective *in vivo* value. The error incurred would be expected to increase with the degree of protein binding of the solute. Consequently it is reasonable to project that highly lipophilic or protein bound solutes may have higher K_{de} values *in vivo* than those calculated from Eq. (20). Protein leakage from the tissue might explain why only a tiny lipid component ($\phi_{lip} = 0.001$, much less than the value suggested by Pearce and Grimmer's, 1972 analysis) was required in Eq. (20) to match the experimental K_{de} values in Table 1. This hypothesis could be tested by *in vitro* studies in which tissue protein levels are preserved by careful sample handling and isolation from the bathing solution by a dialysis membrane.

The partition coefficient K_{de} for testosterone between dermis and buffer solutions was 1.1–2.6 (mean 1.65) when the buffer contained 2% albumin and 5.6–6.4 (mean 6.01) when it did not (Table 3). Approximately 15% of the radiolabel was irreversibly bound to the tissue in these studies. These values indicate that testosterone does bind to dermis components other than albumin; otherwise the K_{de} value from the 2% albumin buffer would have been less than 1 due to exclusion (Bert et al., 1982). The value of K_{de} calculated from Eq. (20) using the estimated f_u value of 0.061 is 4.82 (Table 4). The agreement with the observed mean value of 6.01 ± 0.51 from the albumin-free buffer is reasonable. Thus, the comparison lends a degree of confidence to the use of Eq. (20) to predict dermis/buffer partition coefficients. It is noteworthy that a large variability in experimental K_{de} values was sometimes observed; e.g., testosterone desorption from dermis into PBS yielded $K_{de} = 5.65 \pm 5.06$ for $n = 4$ samples (Table 3, row 4). This variation resulted from high testosterone uptake by one of the samples for which $K_{de} = 13.2$. Despite the high uptake, the D_{de} value obtained by the analysis of the desorption profile for this sample was similar to the other samples. The variation in K_{de} appears to reflect intrinsic variability in tissue properties, possibly in the number of hair follicles or another factor related to lipid content.

Diffusivities in dermis (D_{de}) for 27 skin permeants are reported in Table 1 and plotted as a function of (molecular weight)$^{2/3}$ in Fig. 3a. The plot of log D_{de} versus $MW^{2/3}$ was approximately linear. However, a stronger correlation as well as logical consistency with the physical model for partitioning was obtained by factoring out the effect of binding by means of Eq. (14). The resulting values of D_{free}, that is, diffusivity unencumbered by binding, are shown in Fig. 4b. Over the range of permeants studied, D_{free} had a size dependency consistent with diffusion in a liquid environment. For a given size solute, the absolute value of D_{free} was approximately 3.7-fold lower than diffusivity in water at 37 °C.

A case can also be made for a stronger size dependence for D_{free} than that implied by Eq. (21). A regression of log D_{free} versus $MW^{1/3}$ yielded a slightly better correlation than Eq. (21) (Section 3.3). The degree of improvement becomes even larger if an attempt is made to temperature-correct the diffusivity values to a common temperature of 37 °C. Under the assumption that the viscosity of interstitial fluid in dermis changes with temperature as does that of water, one can estimate the effect of temperature on D_{free} from the Wilke–Chang relationship (Eq. (8)). Precedence for this procedure in collagenous tissues is provided by Bashkatov et al. (2003). Using this approach, the multiplicative correction factors for D_{de} (or D_{free}) values determined at 25 °C or 32 °C that should be applied to correct them to 37 °C are 1.34 and 1.12, respectively. When the data in Tables 1 or 4 are temperature-adjusted in this manner, the major effect is to increase the D_{free} values for the lower molecular weight permeants, since most of these data represent *n*-alkanols studied at 25 °C by Scheuplein and Blank (1973). Regression analysis of the temperature-adjusted dataset (not shown) yielded

$$\log D_{free} = -4.38 - 0.207 \cdot MW^{1/3} \qquad n = 21, \quad s = 0.195, \quad r^2 = 0.718 \tag{22}$$

Eq. (22) may be compared with the power law relationship for the temperature-adjusted dataset (cf. Eq. (21)), which yielded $s = 0.201$, $r^2 = 0.698$. Eq. (22) is presented as a tentative upper limit for the size dependence of diffusivity in dermis, whereas Eq. (21) represents the lower limit. A thorough assessment of these relationships will require more closely controlled studies as well as experimental data for larger permeants. We recommend Eq. (21) as a working model, in part because it allows for greater mobility of serum proteins and of cells which are known to slowly traverse the dermis, albeit by more than purely diffusive mechanisms.

Extrapolation of Eq. (21) to a solute the size of albumin (67.4 kDa) yields $D_{free} = 4.9 \times 10^{-8}$ cm^2 s^{-1}, about 25-fold less than the D_{free} values for the larger solutes in Table 1, but only 3-fold less than the uncorrected D_{de} value for betamethasone valerate. Convective flow due to lymphatic contractions or other mechanical forces could increase the mobility of soluble proteins beyond the purely diffusive value. This comparison reinforces the concept that protein mobility and lymphatic flow should be considered in a transport model for large solutes in the dermis or those that are highly protein-bound.

The dermal clearance values, k_{de}, reported in Table 2 are subject to more uncertainty than the diffusivity and partition values. The k_{de} values were derived from the slopes of *in vivo* skin concentration profiles (Fig. 6), interpreted according to the steady-state limit of a uniformly distributed capillary clearance

model (Eqs. (16) and (17)). The most likely sources of error in this approach are (1) the assumption of uniform clearance with depth and (2) the assumption of a steady-state distribution of permeant in the tissue. The first of these points was discussed in Section 3.4. To investigate the steady-state transport assumption, we conducted a limited investigation of transient transport within the skin for the permeants in Table 2, using the multiple layer diffusion model described in Kretsos et al. (2004). Transport parameters for dermis were taken from the present study, whereas those for stratum corneum were derived from other sources (e.g., Wang et al., 2006, 2007). Epidermis was treated as unperfused dermis, as in Kretsos et al. (2004). The results of these calculations (not shown) confirmed that a true steady-state was most likely not reached for several of the studies reported in Table 2. However, for all permeants but retinoic acid, a pseudo steady-state was reached, leading to a log-linear concentration-depth profile in the dermis, albeit one with a somewhat smaller slope E than predicted from Eq. (17). The maximum departure of E from the steady-state value was 20%. This departure leads to a potential 40% underestimate of k_{de}.

We have noted that there are systematic, i.e., non-random, departures from the exponential decay for several of the datasets in Fig. 6. In our estimation the most promising areas for refinement include: (i) accounting for the spatial dependence of blood concentration in the absorbing capillaries (Dedrick et al., 1982; Gao et al., 1995; Gupta et al., 1995); (ii) development of a more accurate spatial distribution of dermal capillaries that includes follicular structures. These refinements are addressable using microscopic transport models (Kretsos, 2003; Kretsos and Kasting, 2007). The least successful description of dermal concentration according to the distributed model was that of retinoic acid (Fig. 6b). This can be explained in terms of its extremely hydrophobic character ($\log K_{oct} = 6.6$) (Takino et al., 1993) and specific biological functions which lead to facilitated transport in both extracellular and intracellular environments (Allen and Bloxham, 1989). In skin it is thought that extracellular retinoic acid is transported by binding to albumin and (possibly) retinol binding protein, whereas intracellular retinoic acid is transported by the various cellular retinoic acid binding proteins (Siegenthaler and Saurat, 1989). Macromolecule transport in the dermis, as we have argued, may be dominated by convection rather than diffusion. Thus, it is not surprising that the simple passive diffusion and clearance model presented here does not account for retinoic acid distributions in skin.

The decomposition of the E factor with the use of Eq. (16) yielded effective clearance rate coefficients k_{de} in the range $(0.9–14) \times 10^{-4}\ s^{-1}$. Further deconvolution of k_{de} into the microscopic rate constant k_{free} according to Eq. (19) yielded k_{free} values in the range $(2.3–22) \times 10^{-4}\ s^{-1}$. It must be recognized that capillary blood flow is site- and species-dependent and is further influenced by body temperature and the presence of vasoactive agents. Further study of k_{free} would most certainly involve its own decomposition to parameters such as the product of the capillary permeability P_{cap} with the effective exchange surface area S and the blood flow rate Q in the dermis. In the absence of a detailed model for k_{free}, we suggest the use of an analysis initiated for the peritoneum (Dedrick et al., 1982) and later adapted for the study of isolated dermis by Gupta et al. (1995). A comparison of this analysis with ours, assuming that the concentration of the permeant in the tissue is much larger than its post-clearance concentration in the blood phase and that all quantities are volumetrically averaged, yields Eq. (23) which can be used to understand the factors contributing to k_{free}:

$$k_{free} = \left(\frac{1}{P_{cap} \cdot S} + \frac{1}{Q} \right)^{-1} \tag{23}$$

In the limit of a capillary-permeability-limited clearance $k_{free} = P_{cap}S$, while in the limit of a blood-flow-limited clearance $k_{free} = Q$. The pattern exhibited in Fig. 7 suggests that both capillary permeability and blood flow have a role in determining k_{free}. The more lipophilic permeants, which would be expected to have higher values of P_{cap}, tended to have larger values of k_{free} than hydrophilic permeants. Adjustment of the plot to account for ionization (by plotting $f_{non}K_{oct}$ rather than K_{oct} on the abscissa) improved the correlation with respect to piroxicam, but degraded it with respect to salicylic acid. We note that, unlike the other compounds, salicylic acid was applied (as sodium salicylate) to de-epidermized skin rather than to intact skin (Singh and Roberts, 1993b). It seems possible that increased skin blood flow resulting from the surface wound accounts for the high intrinsic clearance rate in this study.

Although the limited data in this analysis do not support a detailed model for the intrinsic clearance constant k_{free}, some degree of estimation is possible. If we consider testosterone to have a blood-flow-limited clearance (a reasonable assumption for a small, lipophilic permeant), then an estimate $Q = 22 \times 10^{-4}\ s^{-1}$ in hairless rat may be derived from these data using Eq. (23). Note that Q and $P_{cap}S$ are per-tissue-volume quantities which explains their units, e.g., the units of Q are derived from (cm^3 of blood s^{-1})/(cm^3 of tissue). This value may be compared with the values $Q = (8–20) \times 10^{-4}\ s^{-1}$ for the magnitude of cutaneous blood flows measured at various anatomical sites of Sprague–Dawley rats by laser Doppler velocimetry (Monteiro-Riviere et al., 1990). The latter values are obtained from the original source after conversion of units, assuming a dermis density of $1.075\ g/cm^3$ (Altshuler et al., 2005). The agreement is quite good. A similar argument would place a lower limit of $Q = 17 \times 10^{-4}\ s^{-1}$ for human volar forearm skin based on the hydrocortisone data in Fig. 6a (Zesch and Schaefer, 1975). By assuming $Q = 22 \times 10^{-4}\ s^{-1}$ in rat, values of $P_{cap}S$ for the less rapidly cleared solutes in Fig. 7 may be deduced from their k_{free} values and Eq. (23). This procedure yields $P_{cap}S = 4 \times 10^{-4}\ s^{-1}$ for piroxicam, $(3–20) \times 10^{-4}\ s^{-1}$ for didanosine and $72 \times 10^{-4}\ s^{-1}$ for methoxsalen. For comparison, $P_{cap}S$ values of $4.2 \times 10^{-4}\ s^{-1}$ and $6.6 \times 10^{-4}\ s^{-1}$, respectively, for Vitamin B_{12} and Cr-EDTA in rabbit skin may be inferred from Paaske's work as summarized in Table 4 of Kretsos and Kasting (2005). Thus, the $P_{cap}S$ values estimated from Eq. (23) are similar to those obtained by different methods. A great deal is known about the values of $P_{cap}S$ in tissues other than skin. We refer the reader to (Kretsos and Kasting, 2005) for a review of this subject as it pertains to skin. This treatment may prove very useful for an order-of-magnitude initial assessment of a

permeant's clearance potential. However, a more physiologically accurate model should account for singular features of the dermal capillary bed such as the geometry of the capillary loop and the convective transport processes which may prove important in conjunction with substantial protein binding (Kretsos and Kasting, 2005).

Further steps toward a more quantitative determination of dermal transport should include a more systematic measurement of diffusivities and partition coefficients, including careful retention of diffusible proteins in the dermis and an investigation of the impact of freezing and heat separation on the measurements. This will minimize the variability due to different laboratories and/or experimental methods. Direct measurement of the protein binding properties of the permeants of interest in albumin solutions of an appropriate concentration, perhaps 2.7% (Bert et al., 1986), should be conducted. Our experience in trying to extend the Yamazaki and Kanaoka (2004) calculation to the larger database presented by Kratochwil et al. (2002) has not been reassuring. Finally, to fully understand transport in the lower skin layers the properties of viable epidermis, which has a structure substantially different from dermis, should be separately evaluated. This is a considerable technical challenge (Khalil et al., 2006).

In this paper, the exponential decay of dermal concentrations with depth characteristic of a uniformly distributed capillary clearance was further established through the analysis of published *in vivo* data. A simple method of identifying the key underlying processes and their characterizing parameters was employed. Estimates for the values of the dermal transport coefficients were presented. Further systematic studies are needed for the clarification of (a) the restriction on diffusion imposed by the dermis; (b) the protein binding effect on both transport and clearance mechanisms; (c) the details of the relationship between dermal clearance coefficient, capillary permeability, and blood flow.

Acknowledgements

We thank Johannes Nitsche for guidance regarding decomposition of the clearance rate constant. Financial support was provided by NIOSH grant R01 OH007529 and by a grant from COLIPA A.I.B.S.

References

Allen, J.G., Bloxham, D.P., 1989. The pharmacology and pharmacokinetics of the retinoids. Pharmac. Ther. 40, 1–27.

Altshuler, G., Smirnov, M., Yaroslavsky, I., 2005. Lattice of optical islets: a novel treatment modality in photomedicine. J. Phys. D: Appl. Phys. 38, 2732–2747.

Amsden, B.G., Goosen, M.F.A., 1995. Transdermal delivery of peptide and protein drugs: an overview. AIChE J. 41, 1972–1997.

Anigbogu, A.N.C., Williams, A.C., Barry, B.W., 1996. Permeation characteristics of 8-methoxypsoralen through human skin; relevance to clinical treatment. J. Pharm. Pharmacol. 48, 357–366.

Auton, T.R., Westhead, D.R., Woollen, B.H., Scott, R.C., Wilks, M.F., 1994. A physiologically based mathematical model of dermal absorption in man. Hum. Exp. Toxicol. 13, 51–60.

Bashkatov, A.N., Genina, E.A., Sinichkin, Y.P., 2003. Glucose and mannitol diffusion in human dura mater. Biophys. J. 85, 3310–3318.

Bauerova, K., Matušová, D., Kassai, Z., 2001. Chemical enhancers for transdermal drug transport. Eur. J. Drug Metab. Pharmacokinet. 26, 85–94.

Benowitz, N.L., Peyton, J., Olsson, P., Johansson, C.-J., 1992. Intravenous nicotine retards transdermal absorption of nicotine: evidence of blood flow-limited percutaneous absorption. Clin. Pharmacol. Ther. 52, 223–230.

Bert, J.L., Mathieson, J.M., Pearce, R.H., 1982. The exclusion of human serum albumin by human dermal collagenous fibres andd within human dermis. Biochem. J. 201, 395–403.

Bert, J.L., Pearce, R.H., Mathieson, J.M., 1986. Concentration of plasma albumin in its accessible space in postmortem human dermis. Microvasc. Res. 32, 211–223.

Bookout, R.L., Quinn, D.W., McDougal, J.N., 1997. Parallel dermal subcompartments for modeling chemical absorption. SAR QSAR Environ. Res. 7, 259–279.

Borsadia, S., Ghanem, A.-H., Seta, Y., Higuchi, W.I., Flynn, G.L., Behl, C.R., Shah, V.P., 1992. Factors to be considered in the evaluation of bioavailability and bioequivalence of topical formulations. Skin Pharmacol. 5, 129–145.

Braverman, I.M., 1997. The cutaneous microcirculation: ultrastructure and microanatomical organization. Microcirculation 4, 329–340.

Cooper, E.R., 1974. Effect of adsorption on membrane diffusion. J. Colloid Interface Sci. 48, 516–517.

Cross, S.E., Anissimov, Y.G., Magnusson, M., Roberts, M.S., 2003a. Bovine-serum-albumin-containing receptor phase better predicts transdermal absorption parameters for lipophilic compounds. J. Invest. Dermatol. 120, 589–591.

Cross, S.E., Magnusson, M., Winckle, G., Anissimov, Y.G., Roberts, M.S., 2003b. Determination of the effect of lipophilicity on the *in vitro* permeability and tissue characteristics of topically applied solutes in human skin layers. J. Invest. Dermatol. 120, 759–764.

Cross, S.E., Roberts, M.S., 1999. Defining a model to predict the distribution of topically applied growth factors and other solutes in excisional full-thickness wounds. J. Invest. Dermatol. 112, 36–41.

Cussler, E.L., 1997. Diffusion: Mass Transfer in Fluid Systems. Cambridge University Press, Cambridge.

Dedrick, R.L., Flessner, M.F., Collins, J.M., Schultz, J.S., 1982. Is the peritoneum a membrane? ASAIO J. 5, 1–8.

Dollery, C., 1999. Therapeutic Drugs, second ed. Churchill Livingstone, Edinburgh.

Florence, A.T., Attwood, D., 2006. Physicochemical Principles of Pharmacy. Pharmaceutical Press, London, p. 77.

Flynn, G.L., Stewart, B., 1988. Percutaneous drug penetration: choosing candidates for transdermal development. Drug. Dev. Res. 13, 169–185.

Gao, X., Wientjes, M.G., Au, J.L.-S., 1995. Use of drug kinetics in dermis to predict *in vivo* blood concentration after topical application. Pharm. Res. 12, 2012–2017.

Gowrishankar, T.R., Stewart, D.A., Martin, G.T., Weaver, J.C., 2004. Transport lattice models of heat transport in skin with spatially heterogeneous, temperature-dependent perfusion. Biomed. Eng. Online 3, 42.

Gupta, E., Wientjes, M.G., Au, J.L.-S., 1995. Penetration kinetics of 2′-3′-dideoxyinosine in dermis is described by the distributed model. Pharm. Res. 12, 108–112.

Guy, R.H., Hadgraft, J., Maibach, H.I., 1982. A pharmacokinetic model for percutaneous absorption. Int. J. Pharm. 11, 119–129.

Higaki, K., Asai, M., Suyama, T., Nakayama, K., Ogawara, K., Kimura, T., 2002. Estimation of intradermal disposition kinetics of drugs: II. Factors determining penetration of drugs from viable skin to muscular layer. Int. J. Pharm. 239, 129–141.

Hueber, F., Wepierre, J., Schaefer, H., 1992. Role of transepidermal and transfollicular routes in percutaneous absorption of hydrocortisone and testosterone: *in vivo* study in the hairless rat. Skin Pharmacol. 5, 99–107.

Joshi, A., Raje, J., 2002. Sonicated transdermal drug transport. J. Control. Rel. 83, 13–22.

Kammerau, B., Zesch, A., Schaefer, H., 1975. Absolute concentrations of dithranol and triacetyl-dithranol in the skin layers after local treatment: *in vivo* investigations with four different types of pharmaceutical vehicles. J. Invest. Dermatol. 64, 145–149.

Kammerau, B., Klebe, U., Zesch, A., Schaefer, H., 1976. Penetration, permeation and resorption of 8-methoxypsoralen. Comparative *in vitro* and *in vivo* studies after topical application of four standard preparations. Arch. Dermatol. Res. 255, 31–42.

Kasting, G.B., Bowman, L.A., 1990. DC electrical properties of frozen, excised human skin. Pharm. Res. 7, 134–143.

Kasting, G.B., Barai, N.D., Wang, T.-F., Nitsche, J.M., 2003. Mobility of water in human stratum corneum. J. Pharm. Sci. 92, 2326–2340.

Khalil, E., Kretsos, K., Kasting, G.B., 2006. Glucose partition coefficient and diffusivity in the lower skin layers. Pharm. Res. 23, 1227–1234.

Kimber, I., Gerberick, G.F., Basketter, D.A., 1999. Thresholds in contact sensitization: theoretical and practical considerations. Food Chem. Toxicol. 37, 553–560.

Kratochwil, N.A., Huber, W., Muller, F., Kansy, M., Gerber, P.R., 2002. Predicting plasma protein binding of drugs: a new approach. Biochem. Pharmacol. 64, 1355–1374.

Kretsos, K., 2003. Transport phenomena in the human skin. Ph.D. Thesis. State University of New York at Buffalo, USA.

Kretsos, K., Kasting, G.B., Nitsche, J.M., 2004. Distributed diffusion-clearance model for transient drug distribution within the skin. J. Pharm. Sci. 93, 2820–2835.

Kretsos, K., Kasting, G.B., 2005. Dermal capillary clearance: physiology and modeling. Skin Pharmacol. Physiol. 18, 55–74.

Kretsos, K., Kasting, G.B., 2007. A geometrical model of dermal capillary clearance. Math. Biosci. 208, 430–453.

Kubota, K., Maibach, H.I., 1993. *In vitro* percutaneous permeation of betamethasone and betamethasone 17-valerate. J. Pharm. Sci. 82, 1039–1045.

Kubota, K., Maibach, H.I., 1994. Significance of viable skin layers in percutaneous permeation and its implication in mathematical models: theoretical consideration based on parameters for betamethasone 17-valerate. J. Pharm. Sci. 83, 1300–1306.

Lee, C.M., Maibach, H.I., 2006. Deep percutaneous penetration into muscles and joints. J. Pharm. Sci. 95, 1405–1413.

McCarley, K.D., Bunge, A.L., 2001. Pharmacokinetic models of dermal absorption. J. Pharm. Sci. 90, 1699–1718.

Moffat, A.C., Osselton, M.D., Widdop, B. (Eds.), 2003. Clarke's Analysis of Drugs and Poisons, third ed. Pharmaceutical Press, London.

Monteiro-Riviere, N.A., Bristol, D.G., Manning, T.O., Rogers, R.A., Riviere, J.E., 1990. Interspecies and interregional analysis of the comparative histologic thickness and laser doppler blood flow measurements at five cutaneous sites in nine species. J. Invest. Dermatol. 95, 582–586.

Monteiro-Riviere, N.A., Inman, A.O., Riviere, J.E., McNeill, S.C., Francoeur, M.L., 1993. Topical penetration of piroxicam is dependent on the distribution of the local cutaneous vasculature. Pharm. Res. 10, 1326–1331.

Pearce, R.H., Grimmer, B.J., 1972. Age and the chemical constitution of normal human dermis. J. Invest. Dermatol. 58, 347–361.

Pibouin, M., Zini, R., Nguyen, P., Renouard, A., Tillement, J.P., 1987. Binding of methoxypsoralen to human serum proteins and red blood cells. Brit. J. Dermatol. 117, 207–215.

Poling, B.E., Prausnitz, J.M., O'Connell, J.P., 2001. The Properties of Gases and Liquids, fifth ed. McGraw Hill, New York.

Potts, R.O., Guy, R.H., 1992. Predicting skin permeability. Pharm. Res. 9, 663–669.

Riviere, J.E., Heit, M.C., 1997. Electrically-assisted transdermal drug delivery. Pharm. Res. 14, 687–697.

Roberts, M.S., Cross, S.E., 1999. A physiological pharmacokinetic model for solute disposition in tissues below a topical application site. Pharm. Res. 16, 1392–1398.

Roberts, M.S., Walters, K.A., 1998. The relationship between structure and barrier function in skin. In: Roberts, M.S., Walters, K.A. (Eds.), Dermal Absorption and Toxicity Assessment. Marcel Dekker, New York, pp. 1–42.

Schaefer, H., Zesch, A., 1975. Penetration of vitamin A acid into human skin. Acta Derm. Venereol. Suppl. (Stockh.) 74, 50–55.

Schaefer, H., Stuttgen, G., Zesch, A., Schalla, W., Gazith, J., 1978. Quantitative determination of percutaneous absorption of radiolabeled drugs *in vitro* and *in vivo* by human skin. Curr. Probl. Dermatol. 7, 80–94.

Scheuplein, R.J., Blank, I.H., 1973. Mechanism of percutaneous absorption.IV. Penetration of nonelectrolytes (alcohols) from aqueous solutions and from pure liquids. J. Invest. Dermatol. 60, 286–296.

Scheuplein, R.J., 1978. Skin permeation. In: Jarrett, A. (Ed.), The Physiology and Pathophysiology of the Skin, vol. 5. Academic Press, London, pp. 1693–1730.

Scheuplein, R.J., Bronaugh, R.L., 1983. Percutaneous absorption. In: Goldsmith, L.A. (Ed.), Biochemistry and Physiology of the Skin, vol. II. Oxford University Press, New York, pp. 1255–1295.

Shah, J.C., 1996. Application of kinetic model to *in vitro* percutaneous permeation of drugs. Int. J. Pharm. 133, 179–189.

Siegenthaler, G., Saurat, J.-H., 1989. Retinoid binding proteins and human skin. Pharmacol. Therapeut. 40, 45–54.

Siddiqui, O., Roberts, M.S., Polack, A.E., 1989. Percutaneous absorption of steroids: relative contributions of epidermal penetration and dermal clearance. J. Pharm. Biopharm. 17, 405–424.

Singh, P., Roberts, M.S., 1993a. Dermal and underlying tissue pharmacokinetics of salicylic acid after topical application. J. Pharmacokinet. Biopharm. 21, 337–373.

Singh, P., Roberts, M.S., 1993b. Iontophoretic transdermal delivery of salicylic acid and lidocaine to local subcutaneous structures. J. Pharm. Sci. 82, 127–131.

Singh, P., Roberts, M.S., 1996. Local deep tissue penetration of compounds after dermal application: Structure-tissue penetration relationships. J. Pharmacol. Exp. Ther. 279, 908–917.

Sommer, A., Lucassen, G.W., Houben, A.J.H.M., Neumann, M.H.A., 2003. Vasoconstrictive effect of topical applied corticosteroids measured by laser Doppler imaging and reflectance spectroscopy. Microvasc. Res. 65, 152–159.

Takino, T., Nakajima, C., Takakura, Y., Sezaki, H., Hashida, M., 1993. Controlled biodistribution of highly lipophilic drugs with various parenteral formulations. J. Drug Target 1, 117–124.

Tojo, K., Chiang, C.C., Chien, Y.W., 1987. Drug permeation across the skin: effect of penetrant hydrophilicity. J. Pharm. Sci. 76, 123–126.

Wagner, H., Kostka, K.-H., Lehr, C.-M., Schaefer, U.M., 2002. Human skin penetration of flufenamic acid: *In vivo*/*in vitro* correlation (deeper skin layers) for skin samples from the same subject. J. Invest. Dermatol. 118, 540–544.

Wang, T.-F., Kasting, G.B., Nitsche, J.M., 2006. A multiphase microscopic model for stratum corneum permeability. I. Formulation, solution and illustrative results for representative compounds. J. Pharm. Sci. 95, 620–648.

Wang, T.-F., Kasting, G.B., Nitsche, J.M., 2007. A multiphase microscopic model for stratum corneum permeability. II. Estimation of physicochemical parameters and application to a large permeability database. J. Pharm. Sci., doi:10.1002/jps.2007, in press.

Wheeler, M.J., 1995. The determination of bio-available testosterone. Ann. Clin. Biochem. 32, 345–357.

Wiig, H., Kolmannskog, O., Tenstad, O., Bert, J.L., 2003. Effect of charge on interstitial distribution of albumin in rat dermis in vitro. J. Physiol. 550, 505–514.

Yamazaki, K., Kanaoka, M., 2004. Computational prediction of the plasma protein-binding percent of diverse pharmaceutical compounds. J. Pharm. Sci. 93, 1480–1494.

Yu, C.D., Fox, J.L., Ho, N.F.H., Higuchi, W.I., 1979. Physical model evaluation of topical prodrug delivery—simultaneous transport and bioconversion of vidarabine-5′-valerate II: parameter determinations. J. Pharm. Sci. 68, 1347–1357.

Yu, C.D., Higuchi, W.I., Ho, N.F.H., Fox, J.L., Flynn, G.L., 1980. Physical model evaluation of topical prodrug delivery—simultaneous transport and bioconversion of vidarabine-5′-valerate III: permeability differences of vidarabine and *n*-pentanol in components of hairless mouse skin. J. Pharm. Sci. 69, 770–772.

Zesch, A., Schaefer, H., 1975. Penetrationskinetik von radiomarkiertem hydrocortisone aus verschiedenartigen salbengrundlagen in die menschliche haut. Arch. Dermatol. Res. 252, 245–256.